24th IAEA Fusion Energy Conference, San Diego CA, October 2012

Numerical Simulations of NBI-driven GAE modes in L-mode and H-mode Discharges in NSTX

E. V. Belova, N. N. Gorelenkov, E. D. Fredrickson,
H. L. Berk, G.J. Kramer, S.S. Medley

NSTX-U

PPPL
PRINCETON PLASMA PHYSICS LABORATORY

Abstract

Hybrid 3D code HYM has been used to investigate properties of beam ion driven GAE modes in NSTX. The HYM code is a nonlinear, global stability code in toroidal geometry, which includes fully kinetic ion description. Excitation of GAE modes have been studied for L-mode and H-mode NSTX discharges. Equilibrium profiles and plasma parameters have been chosen to match several of the NSTX discharge numbers profiles, and the HYM equilibrium solver has been modified to improve the equilibrium fit to the TRANSP and EFIT profiles. Numerical simulations for H-mode have been performed for the NSTX shots, where a GAE activity and related High-Energy Feature (HEF) have been observed. HYM simulations comparison with experimental results for NSTX L-mode shots, show good agreement in terms of the most unstable toroidal mode numbers, frequency, amplitude and the mode structure. It has been shown that most resonant particles have stagnant orbits, and poloidal structure of the unstable mode is relatively coincident with location of the resonant orbits. Linearized and nonlinear simulations have been performed in order to study in detail resonant wave-particle interaction in order to understand the nonlinear evolution of the instability.

Motivation

• Many sub-cyclotron frequency modes are observed in NSTX during NBI injection. These modes were identified as Compressional Alfven Eigenmodes (CAEs) and Global Alfven Eigenmodes (GAEs).

• CAE and GAE modes are predicted to be driven unstable by super Alfvenic NBI ions with $V_b \sim 3V_A$ (90 keV) through the Doppler shifted cyclotron resonance.

• GAE and CAE modes are capable of inducing redistribution of beam ions and strong anomalous electron transport in STs.

• Numerical simulations include: self-consistent anisotropic equilibrium, fully kinetic beam ion description and nonlinear effects.

Correlation between strong GAE activity and enhanced electron transport has been observed in NSTX [Stutman, PRL 2009]

- Plasmas with rapid central electron transport show intense GAE activity (0.5-1.1MHz), while low-transport plasmas are GAE free.
- Flattening of the electron temperature profile with increased beam power.
- Correlation is also observed in experiments with the beam energy scanned between 60keV and 90 keV [Stutman, PRL 2009].
- GAE frequencies are comparable with the trapped electron bounce frequency.
- Measurements of GAE amplitude confirm the central localization of the modes [Tritz, APS 2010].
- Test particle simulations using the ORBIT code predict thermal electron transport due to orbit stochasticity in the presence of multiple core localized GAE modes [Gorelenkov, NF 2010].

- Anomalous electron transport potentially can have significant implications for future fusion devices, especially low aspect ratio tokamaks.

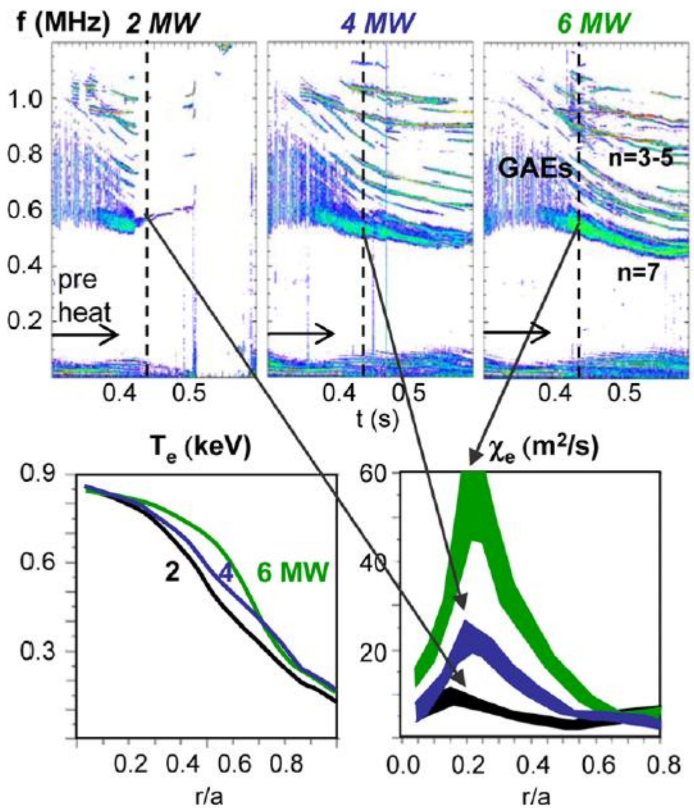

Correlation between GAE activity, T_e flattening, and central electron heat diffusivity χ_e in NSTX H modes with 2, 4, and 6MW neutral beam.

HYM – Parallel Hybrid/MHD Code

HYM code developed at PPPL and used to investigate kinetic effects on MHD modes in toroidal geometry (FRCs and NSTX)

- 3-D nonlinear.
- Several different physical models:
  - Resistive MHD & Hall-MHD.
  - Hybrid (fluid electrons, particle ions).
  - MHD/particle (one-fluid thermal plasma, + energetic particle ions).
- Full-orbit kinetic ions.
- Drift-kinetic electrons.
- For particles: delta-f / full-f numerical scheme.
- Parallel (3D domain decomposition, MPI)[1].

[1]Simulations are performed at NERSC.

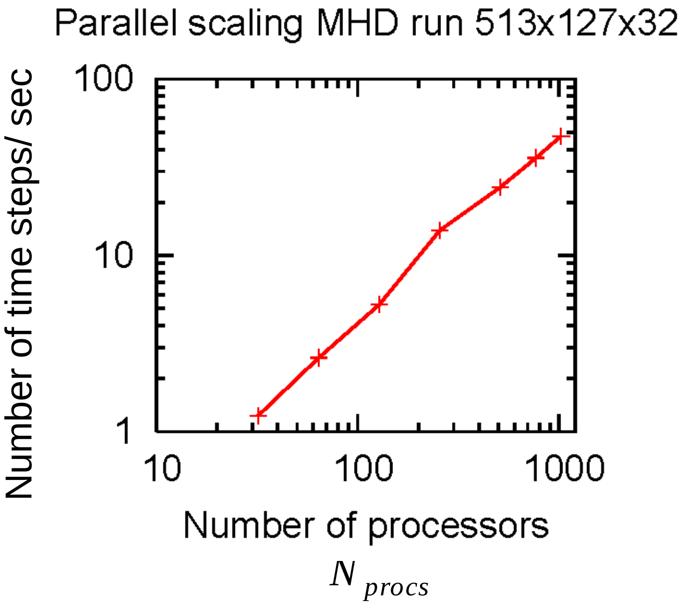

MPI version of HYM code shows very good parallel scaling up to 1000 processors for production-size simulation runs, and allows high-resolution nonlinear simulations.

Self-consistent MHD + fast ions coupling scheme

Background plasma - fluid:

$$\rho \frac{d\mathbf{V}}{dt} = -\nabla p + (\mathbf{j} - \mathbf{j}_i) \times \mathbf{B} - n_i (\mathbf{E} - \eta \mathbf{j})$$

$$\mathbf{E} = -\mathbf{V} \times \mathbf{B} + \eta \mathbf{j}$$

$$\mathbf{B} = \mathbf{B}_0 + \nabla \times \mathbf{A}$$

$$\partial \mathbf{A} / \partial t = -\mathbf{E}$$

$$\mathbf{j} = \nabla \times \mathbf{B}$$

$$\partial p^{1/\gamma} / \partial t = -\nabla \cdot (\mathbf{V} p^{1/\gamma})$$

$$\partial \rho / \partial t = -\nabla \cdot (\mathbf{V} \rho)$$

Fast ions – delta-F scheme:

$$\frac{d\mathbf{x}}{dt} = \mathbf{v}$$

$$\frac{d\mathbf{v}}{dt} = \mathbf{E} - \eta \mathbf{j} + \mathbf{v} \times \mathbf{B}$$

$w = \delta F / F$ - particle weight

$$\frac{dw}{dt} = -(1 - w) \frac{d(\ln F_0)}{dt}$$

$$F_0 = F_0(\varepsilon, \mu, p_\phi)$$

ρ, **V** and p are bulk plasma density, velocity and pressure, n_i and $\mathbf{j}_i$ are fast ion density and current, $n_i << n$ – is assumed.

NSTX-U

PPPL PRINCETON PLASMA PHYSICS LABORATORY

Self-consistent anisotropic equilibrium including the NBI ions

Grad-Shafranov equation for two-component plasma: MHD plasma (thermal) and fast ions [Belova et al, Phys. Plasmas 2003]

$$\frac{\partial^2\psi}{\partial z^2} + R\frac{\partial}{\partial R}\left(\frac{1}{R}\frac{\partial\psi}{\partial R}\right) = -R^2 p' - HH' - GH' + RJ_{i\phi}$$

$$\mathbf{B} = \nabla\phi\times\nabla\psi + h\nabla\phi$$

$$h(R,z) = H(\psi) + G(R,z)$$

$\mathbf{J}_{ip} = \nabla G\times\nabla\phi$, G – poloidal stream function

Fast ions – delta-f scheme: $F_0=F_0(\varepsilon,\mu,p_\varphi)$, where μ is calculated up to 1st order in ρ_i /L; F_0 is chosen to match the distribution functions computed from the TRANSP code (L-mode discharges).

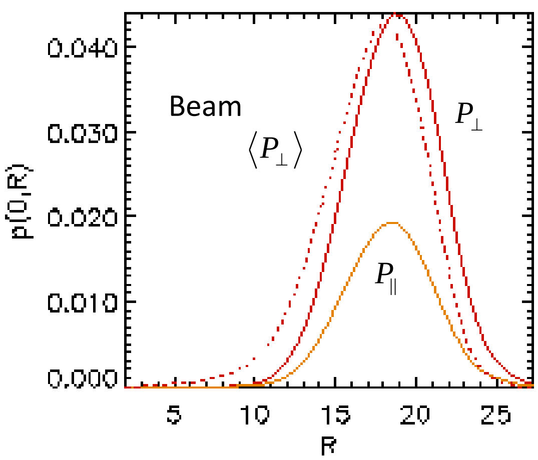

The prompt-loss condition, anisotropy, the large Larmor radius of the beam ions and the strong pitch-angle scattering at low energies have been included in order to match the distribution functions computed from the TRANSP code.

Strong modifications of equilibrium profiles due to beam ions: more peaked current profile, anisotropic pressure, increase in Shafranov shift – indirect effect on stability.

Equilibrium calculations

Equilibrium distribution function $F_0 = F_1(v)F_2(\lambda)F_3(p_\phi)$

$$
\begin{aligned}
F_1(v) &= \frac{1}{v^3 + v_*^3}, \quad \text{for} \quad v < v_0 \\
F_2(\lambda) &= \exp(-(\lambda - \lambda_0)^2/\Delta\lambda^2) \\
F_3(p_\phi) &= \frac{(p_\phi - p_0)^\beta}{(R_0 v - \psi_0 - p_0)^\beta}, \quad \text{for} \quad p_\phi > p_0
\end{aligned}
$$

where $v_0 \approx 3v_A$, $\quad v_* = v_0/\sqrt{3}$, $\quad \lambda = \mu B_0/\varepsilon$ - pitch angle,
$\lambda_0 = 0.8 - 1$,
and $\mu = \mu_0 + \mu_1$ includes first-order corrections [Littlejohn'81]:

$$
\mu = \frac{(\mathbf{v}_\perp - \mathbf{v}_d)^2}{2B} - \frac{\mu_0 v_\parallel}{2B}[\hat{\mathbf{b}} \cdot \nabla \times \hat{\mathbf{b}} - 2(\hat{\mathbf{a}} \cdot \nabla\hat{\mathbf{b}}) \cdot \hat{\mathbf{c}}]
$$

$\mathbf{v}_d$ is magnetic gradient and curvature drift velocity, $\hat{\mathbf{c}} = \mathbf{v}_\perp/v_\perp$,
$\hat{\mathbf{a}} = \hat{\mathbf{b}} \times \hat{\mathbf{c}}$

L-mode simulations: Plasma parameters and profiles are matched to NSTX shot #135419

q-profile

Plasma pressure

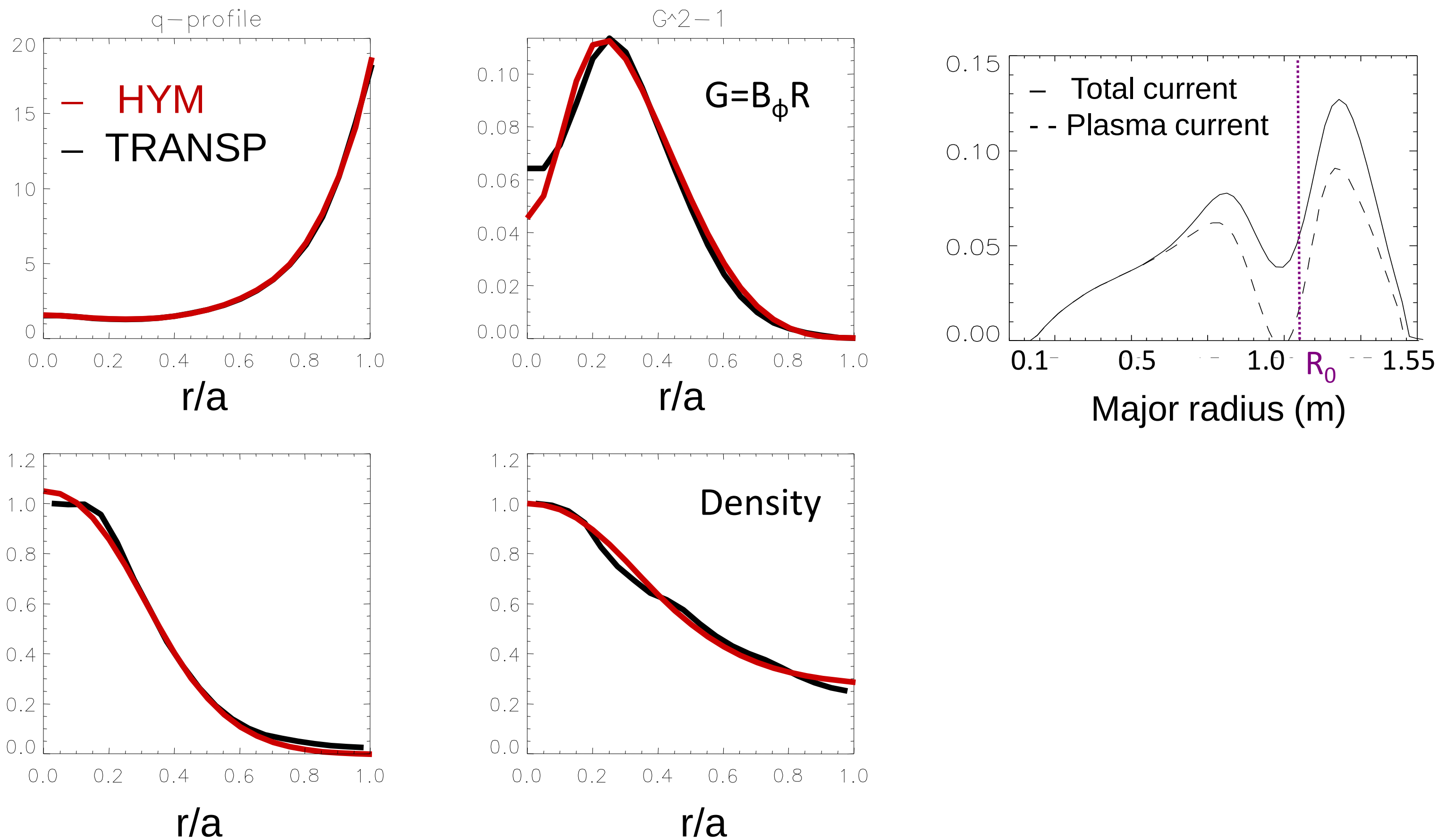

HYM simulations comparison with experimental results for NSTX shot#135419

- Several modes are unstable with toroidal mode numbers n=6 - 9 and frequencies f=0.4-0.8MHz (plasma frame) compared to experimental results of n=7 - 11, and f=0.8-1MHz.
- In the simulations, these modes have been identified as counter-rotating GAE modes based on large perpendicular component of perturbed magnetic field in the core.

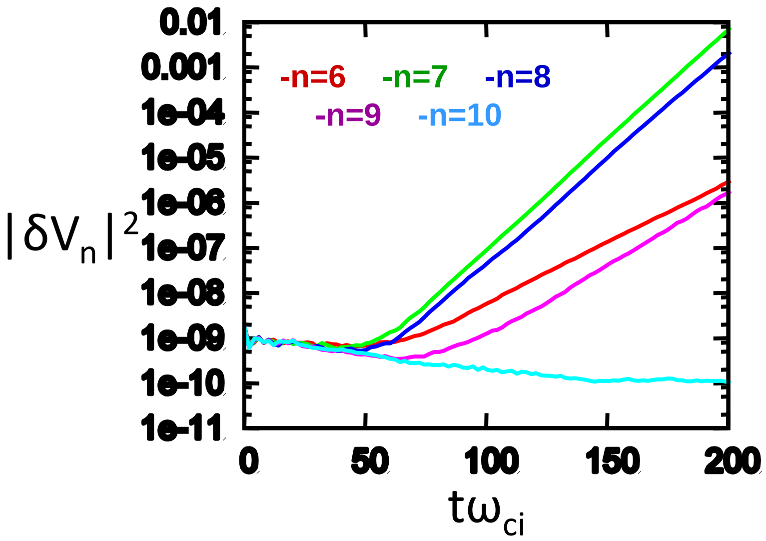

Time evolution of kinetic energy from linearized simulations with n=6-10.

Nonlinear simulations for NSTX shot#135419

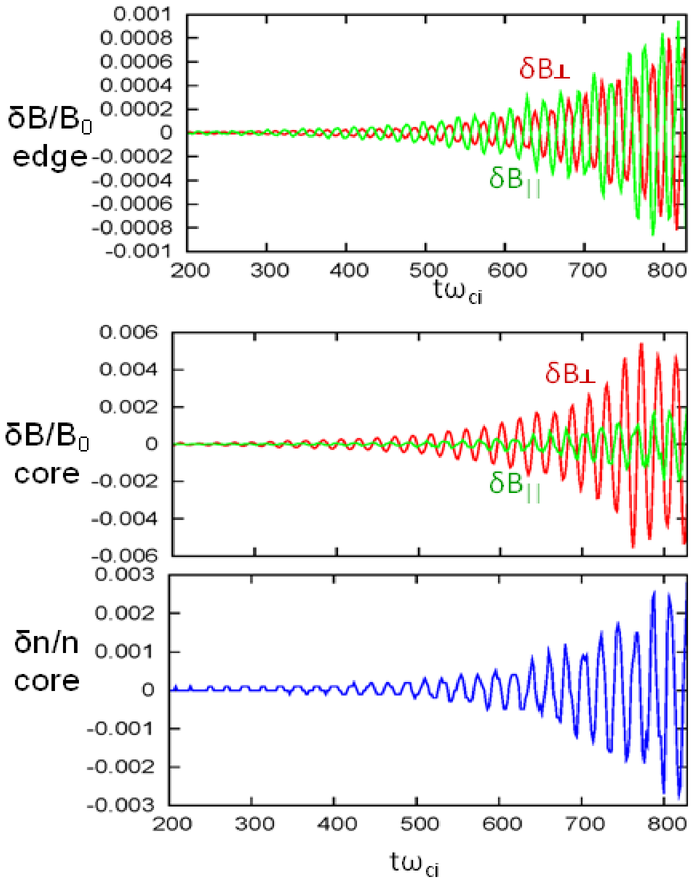

Time evolution of perpendicular and parallel components of magnetic field perturbation and density perturbation from HYM simulations for NSTX shot #135419, GAE mode with $\omega=0.29\omega_{ci0}$, $\gamma=0.01\omega_{ci0}$, (n=9, m=-1).

- For the n=9 GAE mode, mode frequency f =1.02MHz, amplitude δn/n≈0.2%, and linear growth rate γ/ω=3.4% compare with measured mode frequency f≈950 kHz, amplitude δn/n≈0.1%, and estimated growth rate.

- The magnetic perturbations have shear Alfven wave polarization in the core, however they also have significant compressional component with $\delta B_{||}\sim 1/3\cdot\delta B_{\perp}$.

- The compressional component is found to be larger than perpendicular component of δB at the edge, which is also observed in magnetic measurements in NSTX [Fredrickson, NF 2012].

Analysis of resonant wave-particle interaction

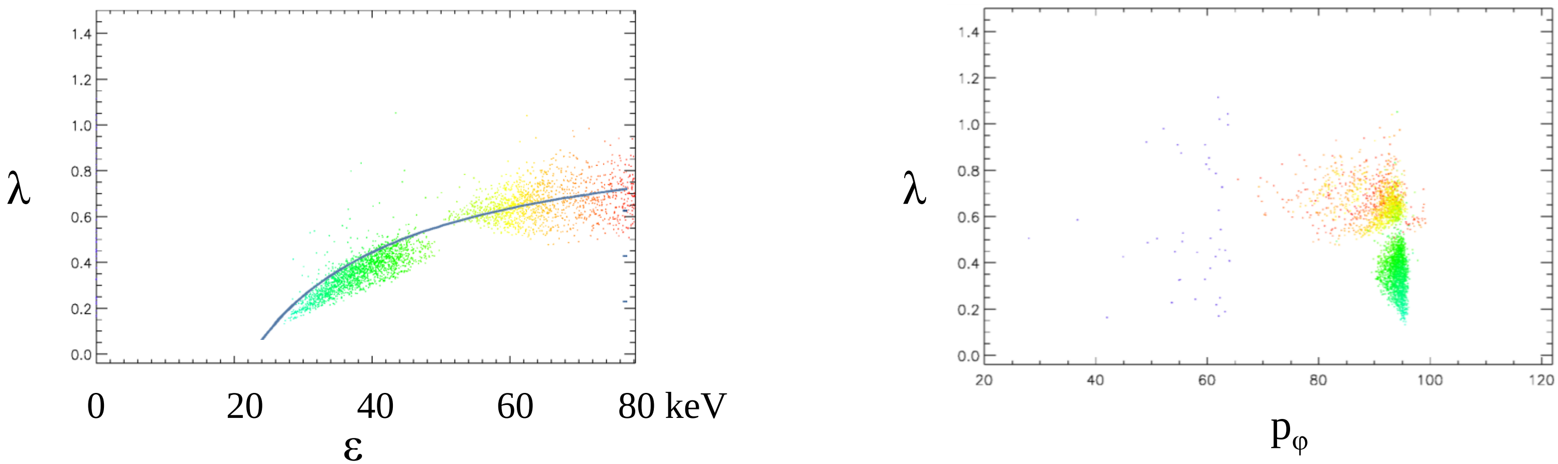

Location of resonant particles in phase space, (a) $\lambda=\mu B_0/\varepsilon$ vs energy, and (b) λ vs toroidal angular momentum $p_\varphi = Rv_\varphi - \psi$. From HYM simulations for NSTX shot #135419, $\omega=0.29\omega_{ci0}$, $\gamma=0.01\omega_{ci0}$, (n=9, m=-1). Solid blue line corresponds to Doppler-shifted cyclotron resonance $\lambda=1- v_{||}^2/2\varepsilon$ for $v_{||} = 1.6V_A$. Particle color corresponds to different energies: from E=0 (purple) to E=80keV (red).

- Resonant particles occupy a wide range of energies.

Analysis of resonant wave-particle interaction

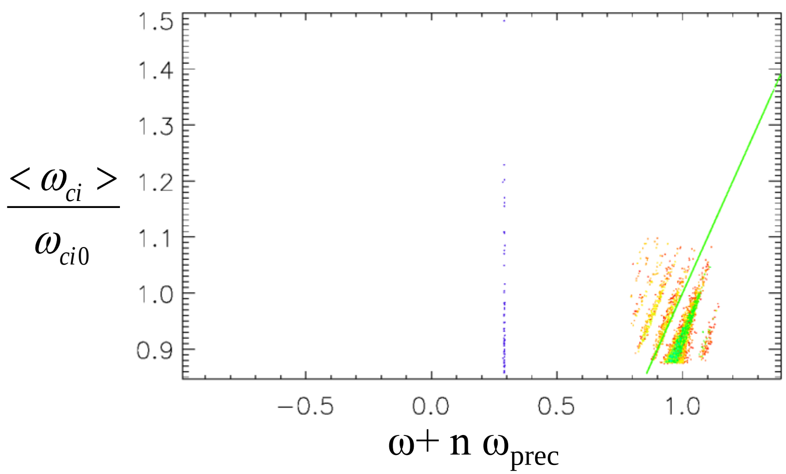

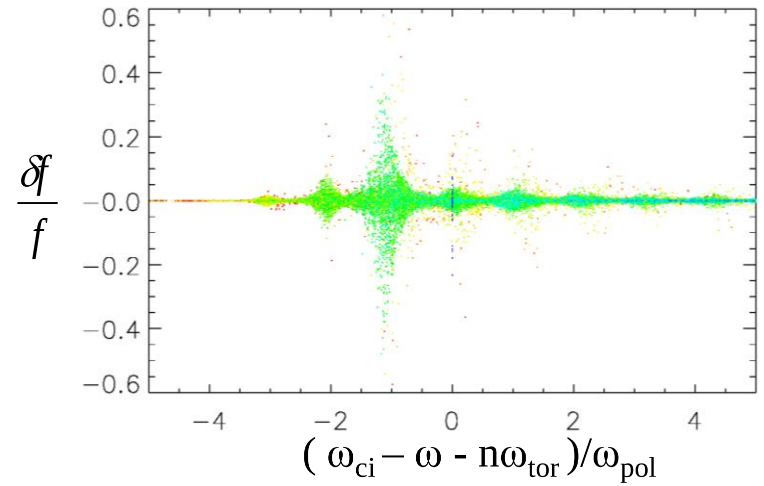

(a) Resonant particles shown with orbit-averaged cyclotron and precession frequencies, both normalized to the ion cyclotron frequency at the axis, ω_{ci0}, (b) Particle weight vs resonant condition. From HYM simulations for NSTX shot #135419, $\omega=0.29\omega_{ci0}$, $\gamma=0.01\omega_{ci0}$, (n=9, m=-1). Particle color corresponds to different energies: from E=0 (purple) to E=80keV (red).

Resonant particles satisfy condition: $\omega - \langle\omega_{ci}\rangle + n\omega_{prec} + k\omega_{transit} = 0$, where n=9, and k=0,±1,±2,… Transit (poloidal) frequency is small compared to other terms in the resonant condition, with $\omega_{transit}$=0.06-0.08 ω_{ci0}, resulting in the fine splitting of resonances.

L-mode simulations: Resonant beam ion orbits

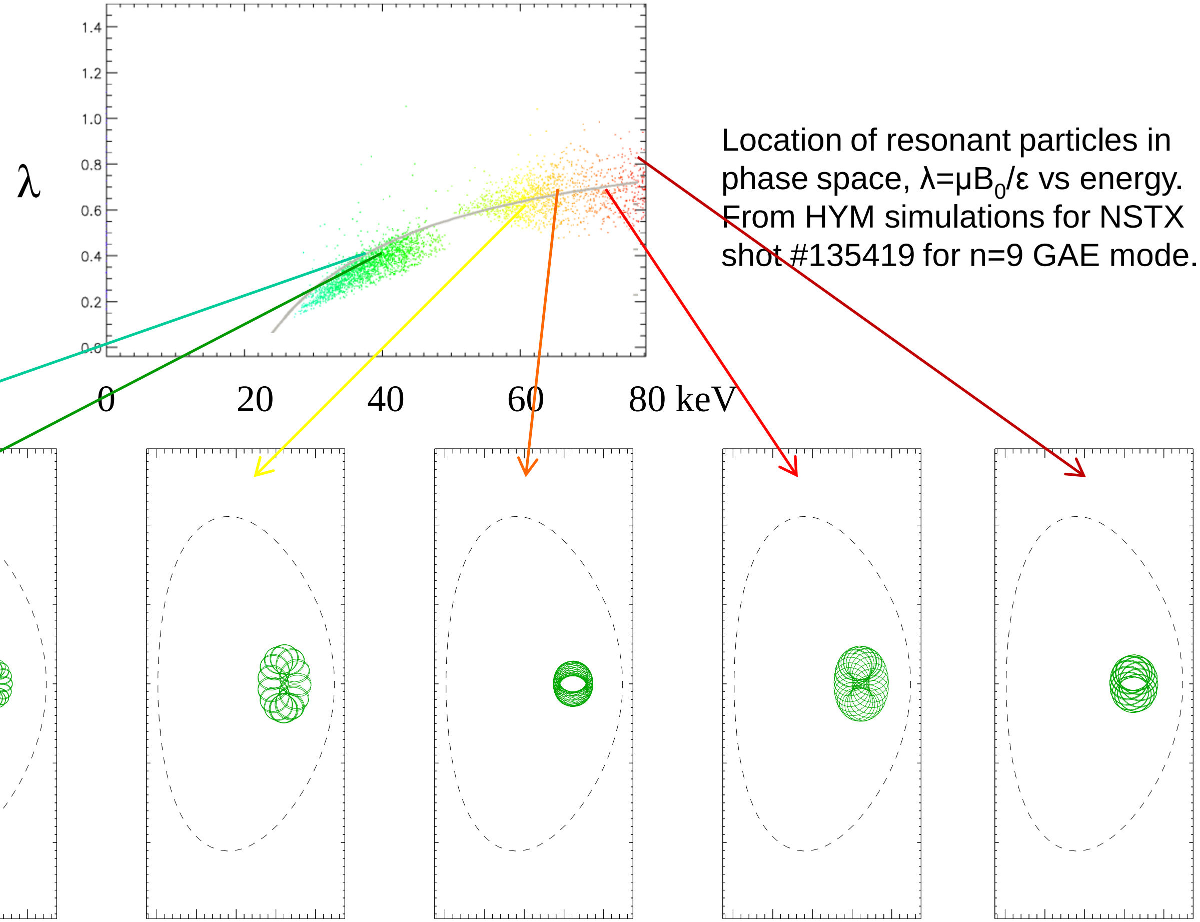

Location of resonant particles in phase space, $\lambda=\mu B_0/\varepsilon$ vs energy. From HYM simulations for NSTX shot #135419 for n=9 GAE mode.

E=38keV, λ=0.38 E=39keV, λ=0.4 E=61keV, λ=0.65 E=64keV, λ=0.69 E=71keV, λ=0.73 E=77keV, λ=0.82

Driving mechanism for GAE modes (n=9)

Delta-f model allows detailed analysis of the instability drive:

$$w = \frac{\delta f}{f}, \quad f = f_0 + \delta f$$

$$\frac{d}{dt}\delta f = -\frac{d}{dt} f_0 = -\underbrace{\frac{d\varepsilon}{dt}\frac{\partial f_0}{\partial \varepsilon}}_{\text{stabilizing}} - \underbrace{\frac{dp_\phi}{dt}\frac{\partial f_0}{\partial p_\phi}}_{\text{stabilizing}} - \underbrace{\frac{d\lambda}{dt}\frac{\partial f_0}{\partial \lambda}}_{\text{destabilizing – responsible for instability}}$$

stabilizing stabilizing destabilizing – responsible for instability

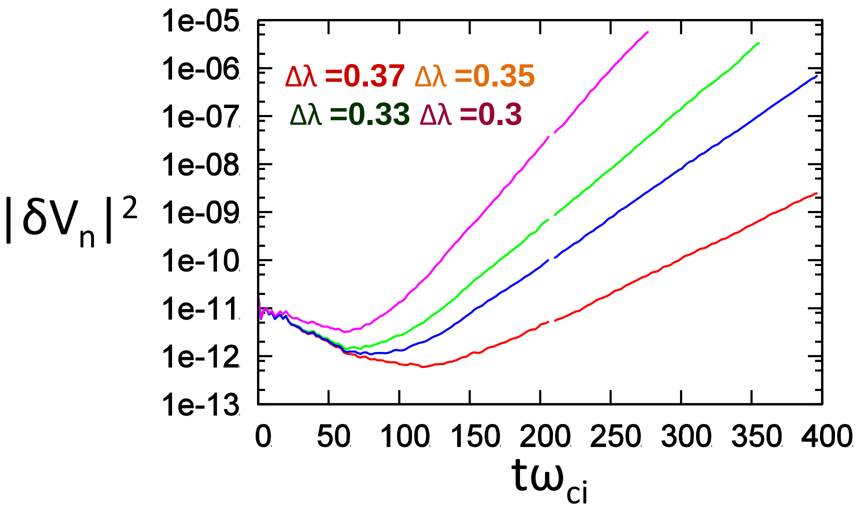

Time evolution of perturbed kinetic energy from linearized simulations with n=9.

Pitch angle distribution has strong effect on the GAE growth rate:

$f_0 \sim \exp[-(\lambda-\lambda_0)^2/\Delta\lambda^2]$, $\lambda = \mu B_0/\varepsilon$

L-mode simulations: GAE mode structure

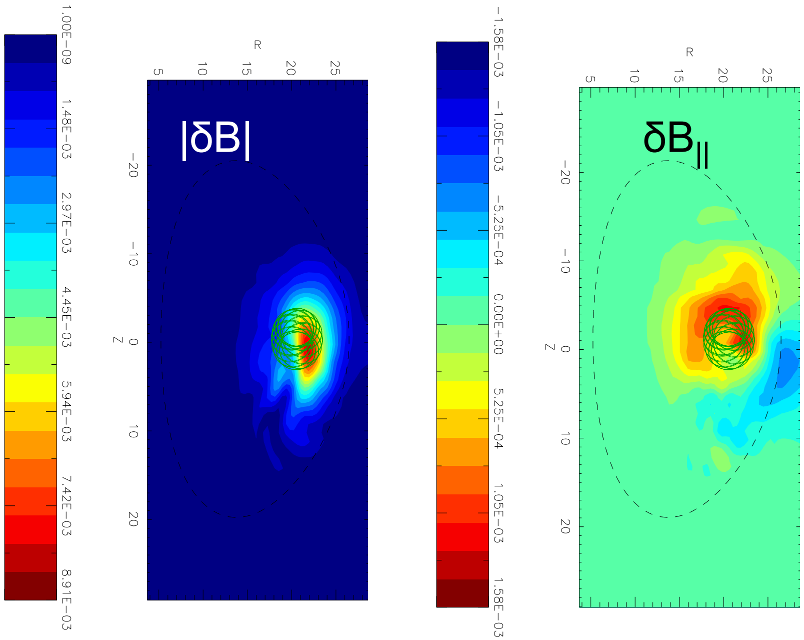

Contour plots of amplitude and parallel components of magnetic field perturbation from HYM simulations for NSTX shot #135419, n=9 GAE mode with $\omega=0.29\omega_{ci0}$, $\gamma=0.01\omega_{ci0}$.

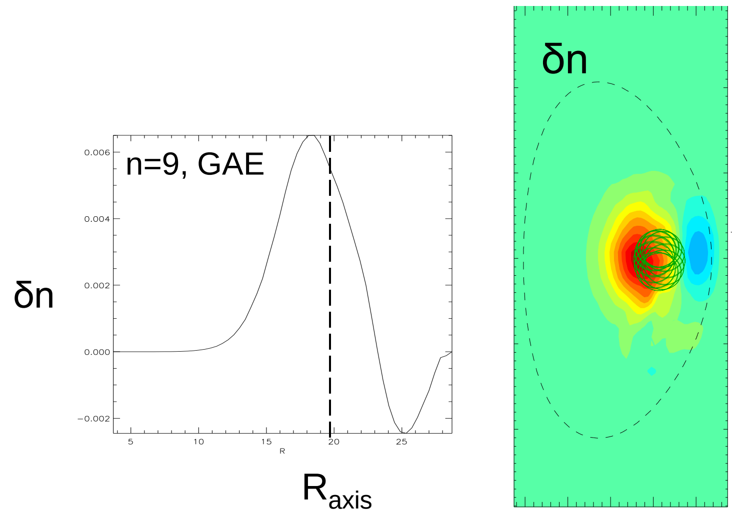

Radial profile and contour plots of density perturbation for n=9 GAE mode.

H-mode simulations: NSTX shot #132800

- In NSTX shot #132800 (I_p = 1.0 MA, B_T = 4.5 kG, E_B = 90 keV), a robust GAE activity and related High-Energy Feature (HEF) have been observed [Medley, NF 2012].

- Simulations show unstable GAE for n ~ 6 – 9, consistent with Mirnov coil data. The n=7, m=-1 GAE mode exhibits the largest growth rate with $\gamma=0.02\omega_{ci0}$ and $\omega=0.21\omega_{ci0}$ (f=600kHz).

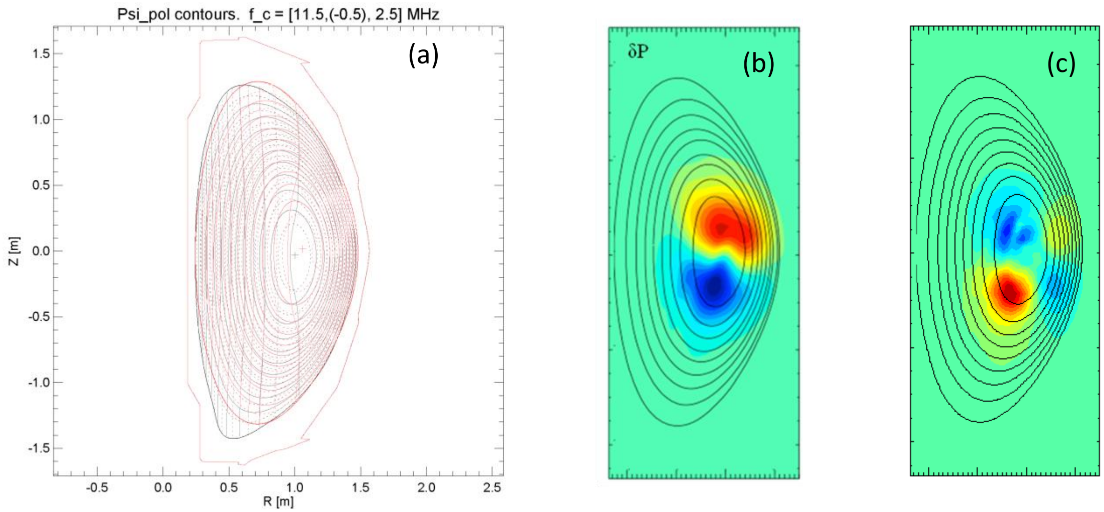

(a) Comparison between EFIT and HYM equilibrium poloidal flux contours and toroidal magnetic field contours; (b) pressure perturbation for n=7,m=-1 and (c) n=6, m=-2 GAE modes from simulations of NSTX shot #132800.

H-mode simulations: NSTX shot #132800

Resonant particle plots, n=7 GAE

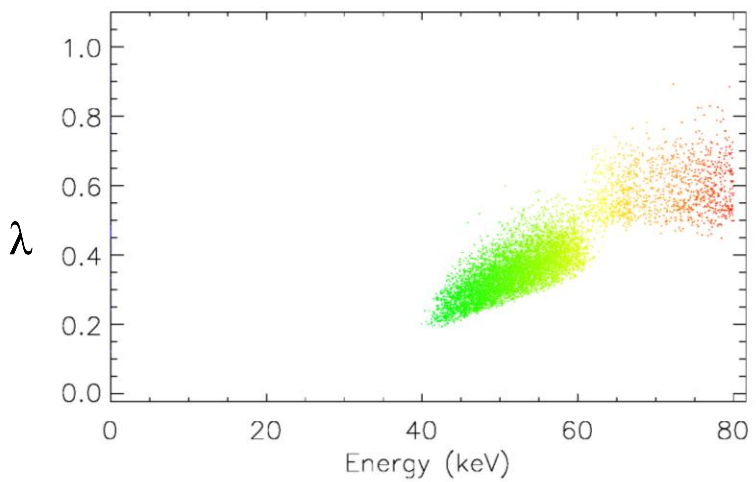

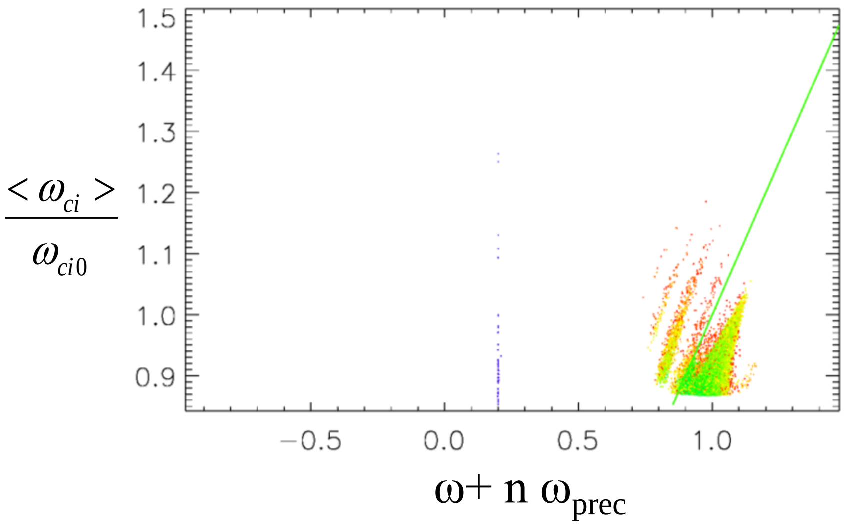

(a) Location of resonant particles in phase space, $\lambda=\mu B_0/\varepsilon$ vs energy, (b) resonant particles shown with orbit-averaged cyclotron and precession frequencies, both normalized to the ion cyclotron frequency at the axis, ω_{ci0}. From HYM simulations for NSTX shot #132800, $\omega=0.20\omega_{ci0}$, $\gamma=0.02\omega_{ci0}$, (n=7, m=-1). Particle color corresponds to different energies: from E=0 (purple) to E=80keV (red). Solid line corresponds to condition $\langle\omega_{ci}\rangle= \omega + n\omega_{prec}$.

H-mode simulations: NSTX shot #132800

Resonant particle plots, n=7 GAE

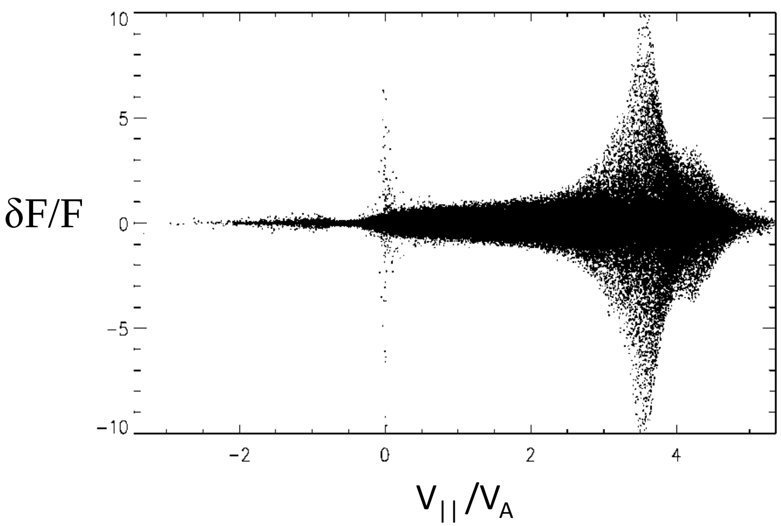

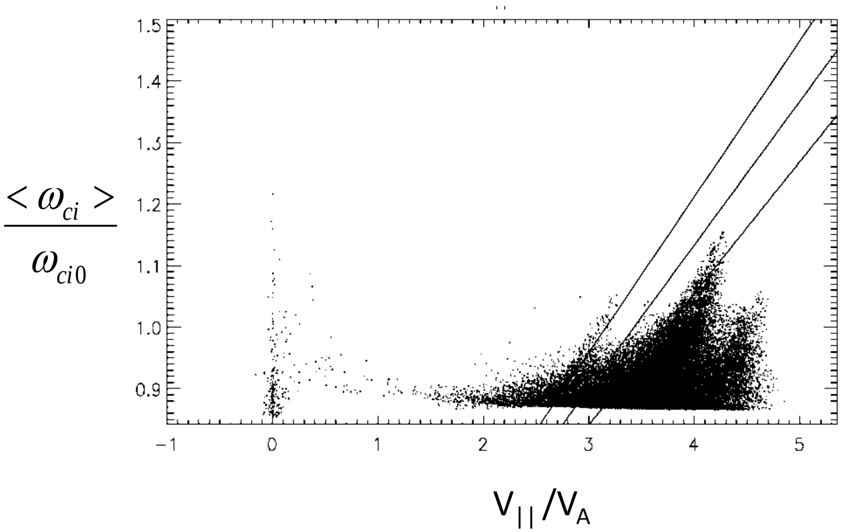

Particle weight w ~ δF/F vs orbit-averaged parallel velocity for all simulations particles. Most resonant particles have $V_{||}/V_A$~3.5.

Orbit-averaged cyclotron frequency vs orbit-averaged parallel velocity for resonant particles. Straight lines correspond to approximate relation:

$$\overline{\omega_{ci}} - \omega = \overline{v_{||}}\,(nq + m')\,/\,q_0 R_0$$

for ω=0.2 and m'= -1,0,1.

GAE and CAE modes observed in NSTX shot # 141398

Experimental measurements

[N. Crocker, IAEA 2012, EX/P6-02]

- Detailed measurements of GAE and CAE modes amplitudes and mode structure were obtained for H-mode plasma in NSTX shot 141398.
- The modes have been identified as CAE modes for frequencies f>600 kHz, and small toroidal mode numbers |n|≤5.
- The modes have been identified as GAEs for f<600 kHz, and |n|~6-8 based on dispersion relations.

HYM simulations

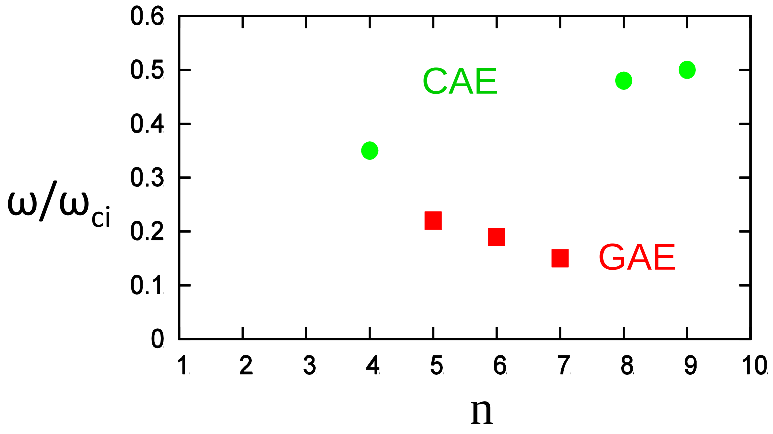

Frequency versus toroidal mode number for most unstable GAE (red) and CAE (green) modes, from HYM simulations for NSTX shot #141398. Frequency is normalized to ion cyclotron frequency at the axis f_{ci}=2.5MHz.

HYM simulations show that most unstable modes for n=5-7 are counter-rotating GAE modes, with shear Alfven wave polarization in the core, and comparable parallel and perpendicular components of perturbed magnetic field at the edge. The n=4 and n=8 and 9 modes are co-rotating CAE modes, which have been identified based on large compressional component of perturbed magnetic field both at the edge and in the core.

H-mode simulations: NSTX shot # 141398

n=4, CAE

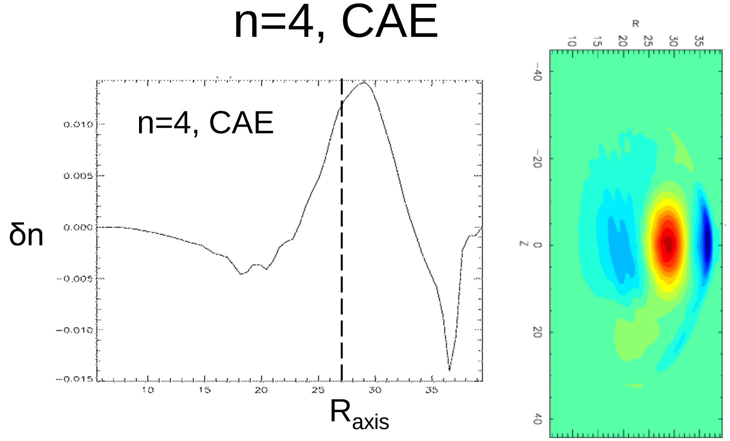

n=5, GAE

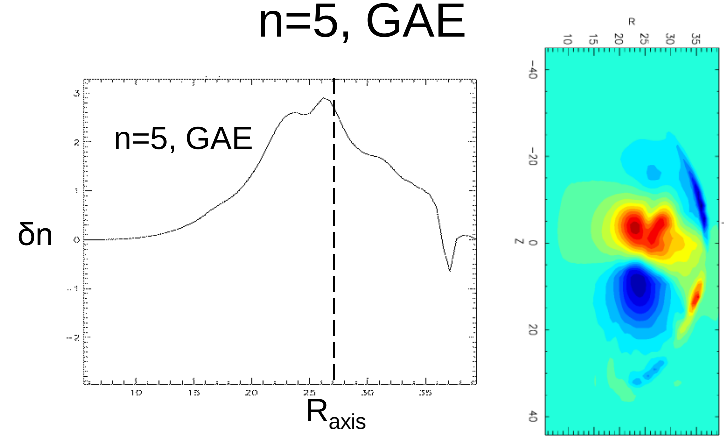

Radial profiles and contour plots of density perturbation for n=4 CAE mode ($\omega=0.35\omega_{ci0}$) and the n=5 GAE mode ($\omega=0.22\omega_{ci0}$). Magnetic axis location is shown by dashed line.

- CAE mode has narrower radial profile compared to GAE, consistent with larger frequency for smaller n and m values.

- For CAEs, $\delta B_{||}$ is significantly larger than $\delta B_{\perp}$ everywhere including the edge, whereas for GAEs, $\delta B_{||}$ is comparable to $\delta B_{\perp}$ only at the edge.

GAE vs CAE mode structure

n=4, CAE

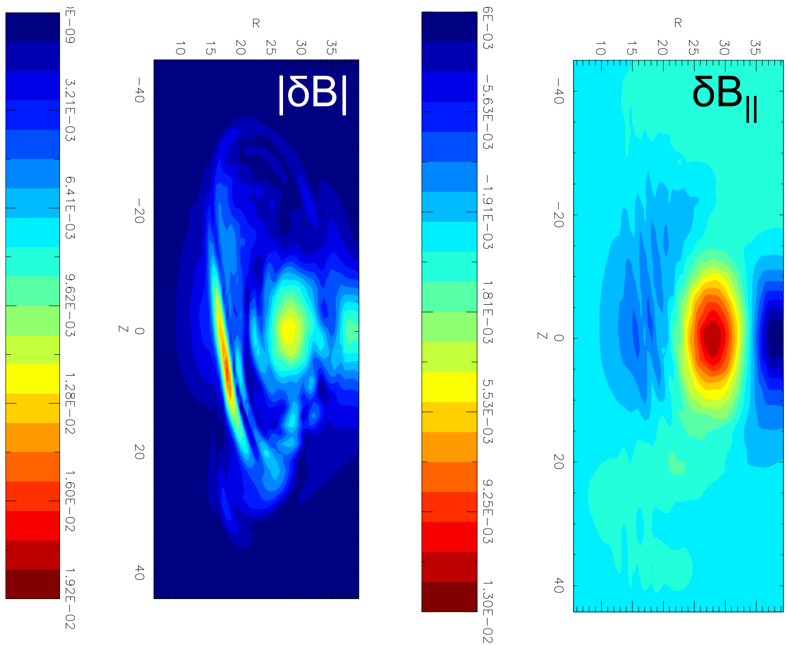

Contour plots of |δB| and parallel components of magnetic field perturbation from HYM simulations of n=4 CAE mode; $\delta B_{||} \sim 0.7\ |\delta B|$.

n=6, GAE

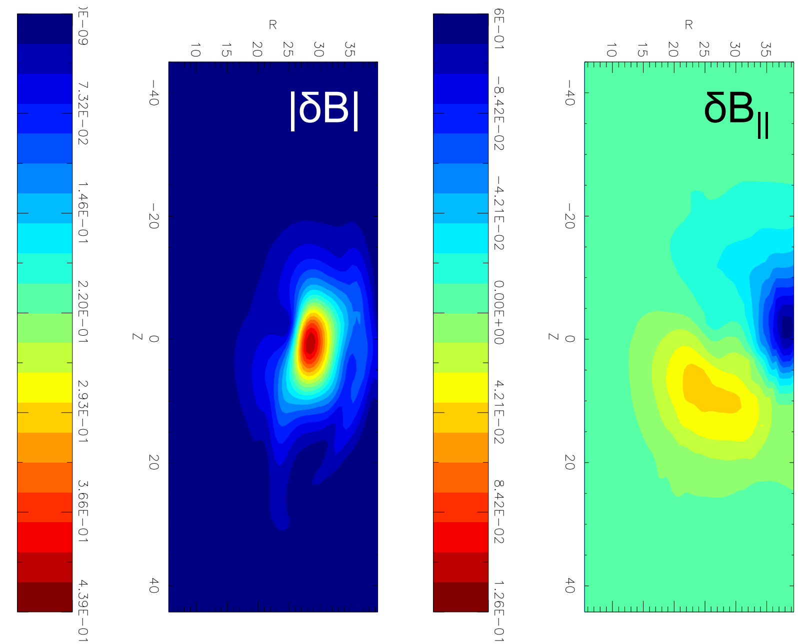

Contour plots of |δB| and parallel components of magnetic field perturbation from HYM simulations of n=6 GAE mode; $\delta B_{||} < 0.3\ |\delta B|$.

H-mode simulations: High-n co-rotating CAE modes

n=8, co-rotating CAE

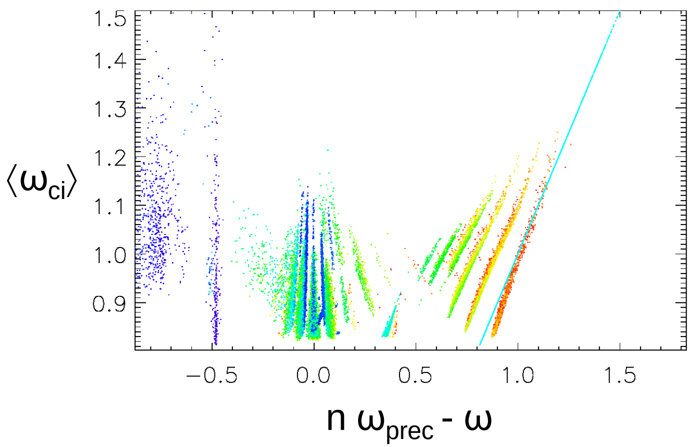

Scatter plot showing orbit-averaged cyclotron and precession frequencies of resonant particles (normalized to the ion cyclotron frequency at the axis, ω_{ci0}). From HYM simulations for NSTX shot #141398 of the n=8 co-rotating CAE mode with $\omega=0.48\omega_{ci}$. Particle colour corresponds to different energies: from E=0 (purple) to E=80keV (red).

- Two groups of resonant particles, one group which satisfy condition: $\omega - k_{||}v_{||} = 0$, and another which satisfy the Doppler-shifted cyclotron resonant condition: $|\omega| + \omega_{ci} - k_{||}v_{||} = 0$.

- In contrast to unstable counter-rotating GAE modes (n=5-7), the Doppler shift is larger than the orbit-averaged cyclotron frequency for the large-n CAE modes.

- Unstable CAE modes have not been observed in the previous L-mode simulations. Conditions favorable for the excitation of these modes are been investigated.

Conclusions

- Excitation of GAE modes have been studied for L-mode and H-mode NSTX discharges. Equilibrium profiles and plasma parameters have been chosen to match several of the NSTX discharge numbers profiles, using the TRANSP and EFIT codes.
- HYM simulations of GAEs show good agreement with experimental results for both NSTX L-mode and H-mode shots, in terms of the most unstable toroidal mode numbers, frequency and the mode structure.
- HYM simulations for L-mode shots show good agreement in terms of the amplitude, and estimated growth rate.
- Linearized and nonlinear simulations have been performed in order to study in detail resonant wave-particle interaction in order to understand the nonlinear evolution of the instability. It has been shown that most resonant particles have stagnant orbits, and poloidal structure of the unstable mode is relatively coincident with location of the resonant orbits.